CITY COLLEGE

CITY UNIVERSITY OF NEW YORK

Final Project

ME 474: Senior Design II

Fall 2011

Design of Porous Track for Air Bourne Jet Train

Sponsor and Client:

Prof. Yiannis Andreopoulos

Instructor:

Prof. Charles B. Watkins

Submitted By:

Group 1

Pradip Thapa, Azhar Patankar, Christopher Carlon, Zahid Khan

January 20, 2012

Executive Summary

This project purpose a design and performance test of an 1:20 scale model of airborne jet train (AJT) that would glide on a soft porous track (SPT) and demonstrate the validation of the proposed new theory explaining the generation of pressure and lift forces in a random soft fibrous media layer under dynamic compaction. The governing equation of model for the pressure distribution is Brinkman equation which is modified form of Darcy equation. The boundary condition for the solution of the Brinkman's equation is that the fiber is confined between two planar sides (no slip walls) on either side where there is no pressure drop by viscous shear effect of or leakage, an infinite horizontal lower boundary and incline upper boundary that is within lubrication limit.

The numerical solution of the governing differential equation for velocity of the 1:20 scale train was evaluated keeping the mass and thrust as variable and the drag coefficient of the body as 0.2. This parametric velocity solution was then incorporated in the non-dimensional solution of Brinkman equation with variable Darcy's permeability given by Carman–Kozeny equation. Finally thorough an iterative process and legitimate consensus was reached between the mass to generate compaction and thrust to produce required speed to generate lift of the model.

Using polyester fiber as fibrous porous material with permeability $3.4*10^{-9}$ m^2, and the compression ratio of 1.5 i.e. ratio of the thickness of porous material at leading edge and the trailing edge. Numerical results showed that for a 20 kg mass of the train powered with 8N thrust produce a speed of 0 to 4 m/s in 10 sec and the lift was observed at speed of 1.52 m/s. The pressure center was found to be constant at 0.7 m from trailing edge of the SKI which is off from mass center by 0.1 m to the trailing side which attributed a pitching moment. This moment can be compensated by counter moment produced by NACA 0012 airfoil at 15 degree angle of attack at the steady state speed of 42 m/s. However, due to the limitation of the resources and scope of the experiment the idea was proposed to manufacture the train in the way that the mass center of the train coincidence with the pressure center eliminating any moment and the numerical results showed the lift occurs at 1.72 m/s with the limit of the track length of 15 meter.

Finally a 1:20 scale model plywood train was constructed with a plywood SKI mounted underneath the train body and two sets of wheel was attached as the undercarriage of the train. The train was attuned to weight around 22 kg and pushed along a track of 30 feet long. The test section was 10 feet of length at mid-section of the track and is equipped with a pressure sensor at the middle of the test section. The data acquisition software and analysis in MatLab gave a result that is the pressure developed was $1/3^{rd}$ of the theoretical value. Due to Safety factor and space constraints in experimental area, rockets were not used to propel the train but the train was pushed by human force and the speed of the train was obtain used various technique to correspond to the theoretical predictions.

Table of Contents

Nomenclature

$x = x - coordinate\ of\ position\ along\ the\ SKI\ planform\ (m)$
$L = length\ of\ the\ SKI\ (m)$
$\tilde{x} = dimensionless\ position$
$h = differential\ thickness\ of\ posrous\ material\ along\ the\ SKI\ planform (m)$
$h_1 = thickness\ of\ porous\ material\ at\ leading\ edge\ (m)$
$h_2 = thickness\ of\ porous\ material\ at\ trailing\ edge\ (m)$
$\tilde{h} = dimensionless\ thickness$
$K_p(h_1) = Darcy'sPermeability\ (m^2)$
$\varepsilon = void\ fraction$
$\mu = dynamic\ viscosity$
$\rho = density\ of\ air\ \left(\frac{kg}{m^3}\right)$
$m = mass\ of\ train\ (kg)$
$W = weight\ of\ the\ train\ (N)$
$A_s = Area\ of\ SKI\ planform\ (m^2)$
$C_D = drag\ Coefficient$
$T = thrust\ (N)$
$A = cross\ sectional\ area\ (m^2)$
$t = time\ (s)$
$F_s = normal\ Compression\ Force\ (N)$
$P(x) = pore\ air\ pressure\ \left(\frac{N}{m^2}\right)$
$F_a = normail\ pore\ air\ force\ (N)$
$R_r = reaction\ on\ rear\ wheel\ (N)$
$R_f = reaction\ on\ front\ wheel\ (N)$
$c = air\ pressure\ centroid\ position\ (m)$

1. Introduction

1.1 Project description

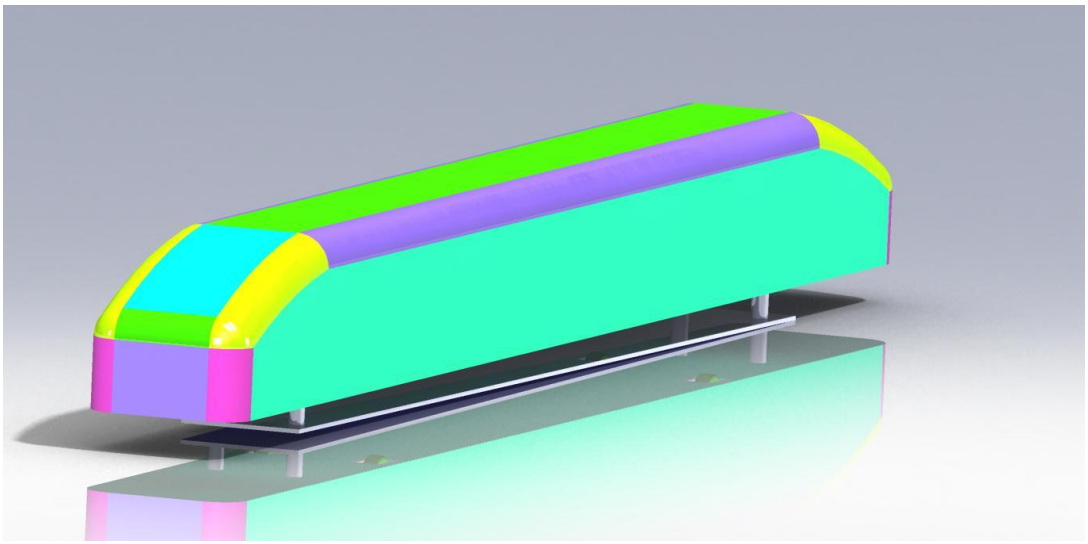

Figure 1.0 Concept Model of Air Jet Train

A proof concept of 1:20 scale model of an Airborne jet train (AJT) with a SKI underneath as shown in figure 1.0 is to be purposed which can demonstrate the lift force generate during dynamic compaction of the fibrous porous medium in a laboratory setup. Initially the train wheels support the train in the track and as the train is propel by the thruster, the ski glides over the porous material at a very small angle of attack such that the trailing edge push the air through the void which eventually created a dynamic pore pressure as predicated by the Brinkman's equation [1]. While the ski of the train will be sliding over a high compressible fibrous material the dynamic pressure builds up under the SKI of the train generates dynamic lift forces. Our goal is to exams these dynamic lift forces being generated. Furthermore we will be checking the design and the performance of this train as well. The supposed length of the track will be around 15-20 meters and it will be made sure that the proposed design would allow lift-off velocities within this limit.

1.2 Motivation

The concept of this design project emerged from the motion of red blood cells through capillaries. Figure 2 describes the effect of increasing velocity of red blood cells through capillaries.

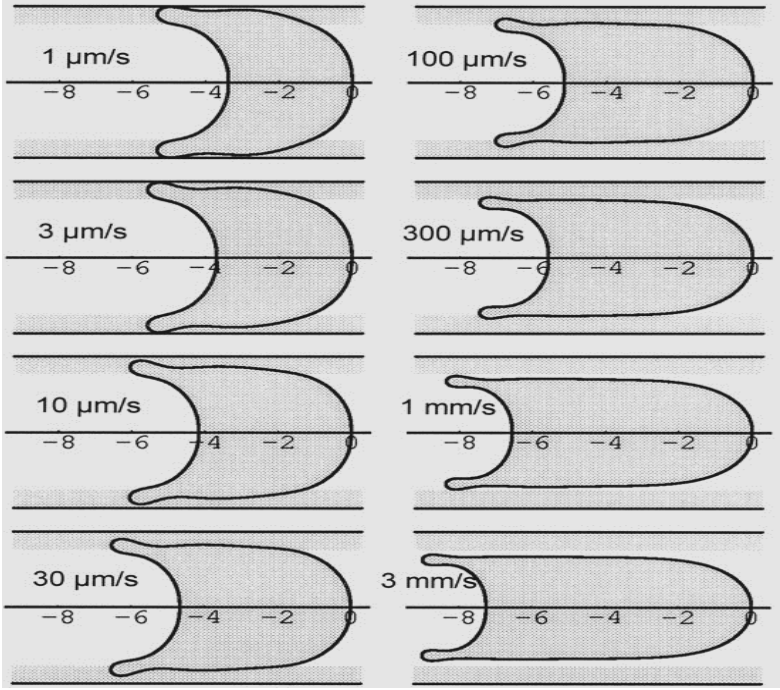

Figure 2.0 Motion of red blood cell in capillaries

It can be observed from the above figure that as the velocity of the red blood cells increases, it shrinks along the y-axis and elongates in the x-axis. This behavior occurs due to the presence of glycocalyx which is a soft porous material. As the velocity of the red blood cells increases, the compression forces exerted by this material on the red blood cell increases. To explain this phenomenon in which a red blood cell quickly lifts off from the surface and glides near the edge of glycocalyx, a new theory was required to explain. This need gave arise to convergence of lubrication theory and Brinkman's equation to describes the flow of fluids (liquids and gases) in a geometry in which one dimension is significantly smaller than the other and pressure variation along the motion of the boundary layer.

1.3 Background

Feng and Weinbaum [J. Fluid Mech. 422, 282 (2000)] have shown a similarity between red blood cell gliding on endothelial surface and glycocalyx(Porous Media) and a human snowboarding on fresh powder snow(Porous Media) and their corresponding pressure gradient along the contact surface. However the classical lubrication theory was not able to explain this phenomenon hence a new theory was proposed and experiment were conducted to verify the pore pressure generated during compaction.

Modeling fluid flow in porous heterogeneous materials with more than one typical pore size is a challenge. One approach is to divide the medium into two regions i.e. larger pores and homogeneous regions of smaller pores.

In larger pores, the Stokes equation for incompressible flow holds

$$\nabla p = \mu \nabla^2 v; \qquad \nabla . v = 0$$

where

p is the pressure

v is the fluid velocity

μ is the fluid viscosity

In smaller pores, the flow is described by Darcy's law. The boundary conditions to be satisfied at the pore/permeable medium interface are continuity of fluid velocity and shear stress. Darcy's law alone is not sufficient to satisfy these boundary conditions. The Brinkman equation, a generalization of the Darcy's law, fully satisfies the above mentioned flow. Brinkman's equation is

$$\nabla \mathrm{p} = -\frac{\mathrm{k}}{\mu}\mathrm{v} + \mu_e \nabla^2 v$$

Where,

μ_e = effective viscosity parameter

This theory is valid in the limit where the structure is so compressible that the normal forces generated by elastic compression of the fibers are negligible compared to the pressure forces generated within the porous layer.

1.4 Literature search

Theoretical Methods:

This study begins with a brief introduction of basic flow geometry for planar lifting surface. Afterwards fundamental of boundary conditions, variable Darcy's permeability and dimensionless parameter parameterization of pressure function with generalized and simplified governing equation.

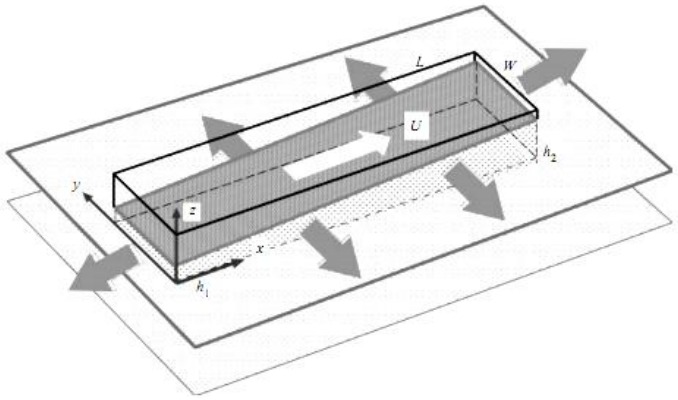

(a)

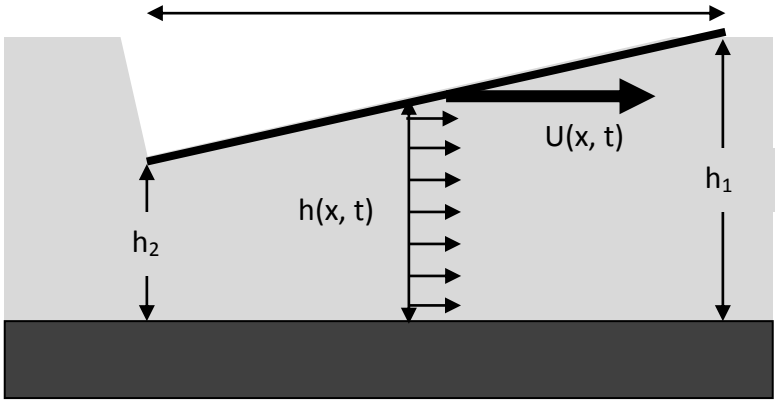

(b)

Figure 3.0 Basic Flow geometry for planar lifting surface. (a) 3D Representation SKI over track. (b) (x, y) coordination system of Flow field.

Introducing the dimensionless variables

$$\tilde{x} = \frac{x}{L} \tag{1}$$

$$\tilde{h} = \frac{h}{h_1} \tag{2}$$

$$\tilde{p} = \frac{pK_p(H_1)}{\mu UL} \tag{3}$$

$$\tilde{k} = \tilde{h} - \tilde{h} * \frac{ln\tilde{h}}{\ln(1-\epsilon)} \tag{4}$$

$$\widetilde{P(x)} = -\int_0^{\tilde{x}} \frac{C_1 + \tilde{h}}{\tilde{k} * \tilde{h}} \tag{5}$$

$$C_1 = \frac{-\int_0^1 \frac{1}{\tilde{k}} d\tilde{x}}{-\int_0^1 \frac{1}{\tilde{k}\tilde{h}} d\tilde{x}} \tag{6}$$

$$\widetilde{dh} = \left(\widetilde{h_1} - \widetilde{h_2}\right) d\tilde{x} \tag{7}$$

A typical drag coefficient is given by, $C_D = \frac{D}{0.5 * \rho * U^2 * A}$

$$D = C_D * 0.5 * \rho * U^2 * A \tag{8}$$

By Newton's second law,

$$m * a = T - D$$

$$m * \frac{du}{dt} = T - C_D * 0.5 * \rho * U^2 * A \tag{9}$$

The compression of the fibers varies linearly for thickness difference of 0.4,

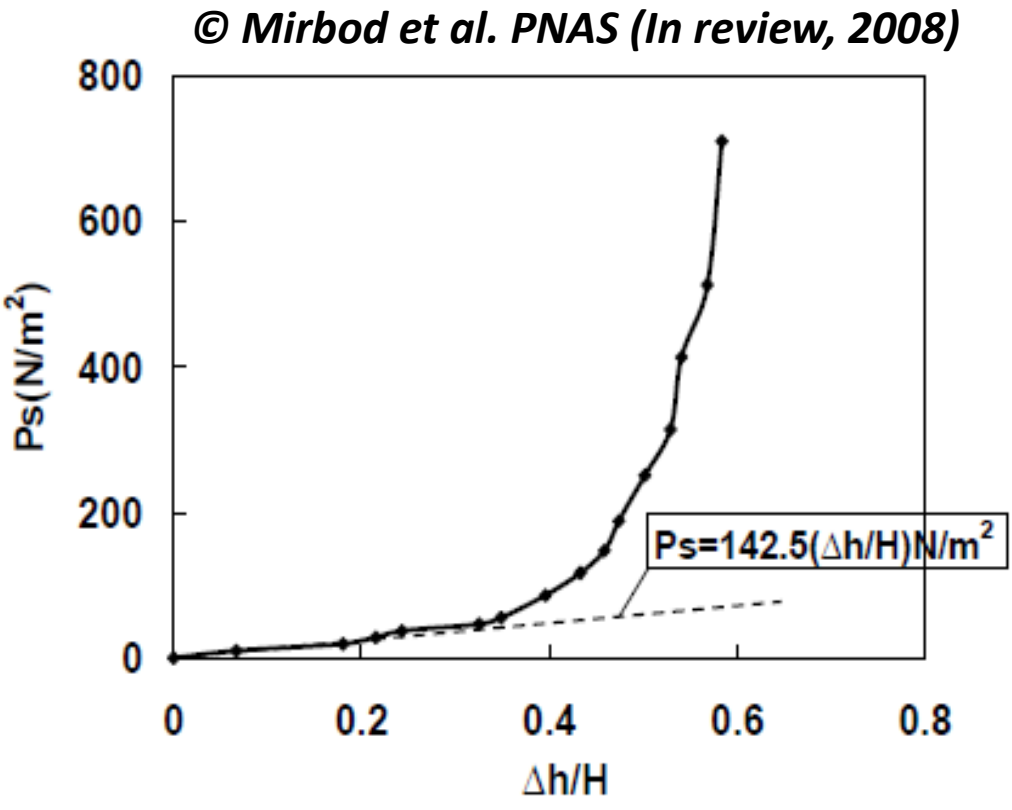

Figure 4.0 Experimental result of quasi compaction of porous material

$$F_s = 142.5 * \frac{h_1 - h_2}{h_1} \quad (10)$$

2. Problem statements and objective

2.1 Objectives

- To examine the generation of dynamic lift forces due to the dynamics pressure distribution under the moving SKI plan form due to the compaction of highly compressible fibrous materials.
- A 1:20 scale model design and performance of an airborne jet train (AJT) that would glide on a soft porous track (SPT).
- The proposed design would allow lift-off at velocities within the limit of length of the track.

2.2 Customer requirements

2.2.1 Product Design Specifications

Air Jet Train	
Parameters	**Estimated**
The thrust used for propulsion (N)	10-15
Propulsion System	Solid state fuel Rocket
Mass of the train (kg)	15-25
Airfoil at the front of train	Yes
Aerodynamic Body (body drag coefficient)	0.2

Soft Porous Track	
Parameters	**Estimated**
Length of the track (m)	15-20
Lateral air leakage form side boundary	No
$\frac{\text{Thickness of porous material}}{\text{length of the ski}}$	<< 1
Polyester Fiber Darcy Permeability (m^2)	3.4*10^-9

Table 1.0 Product Design Specification and Client requirements

2.2.2 Design Process

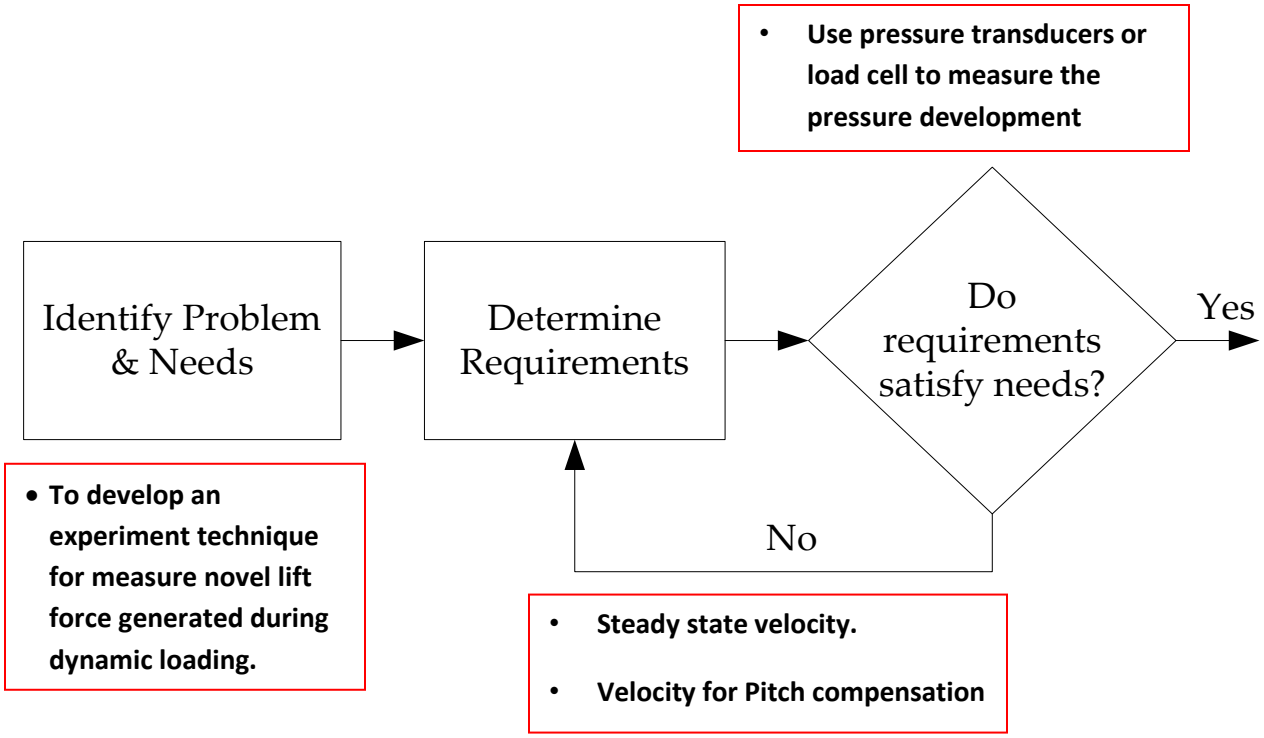

Figure 5.0 Design optimization and Requirement Assessment flow Diagram

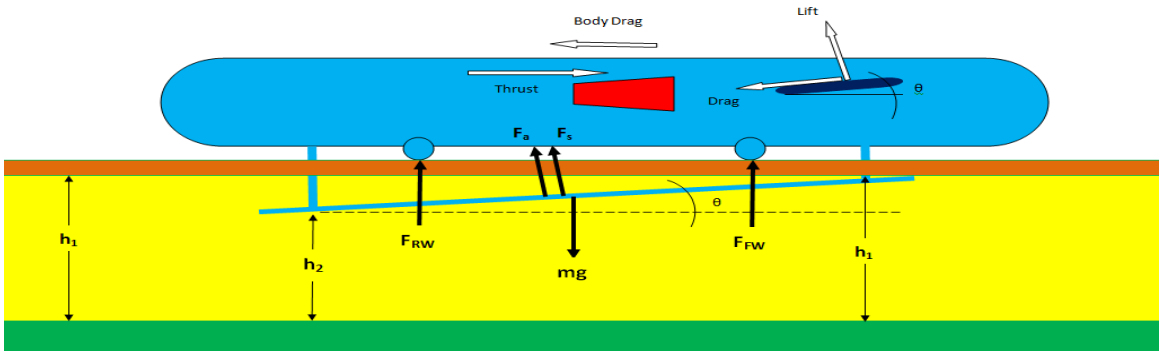

Figure 6.0 Free Body Diagram of forces

In figure 5.0, the flow diagram shows the primary needs of the project is to develop an technique to measure novel lift force generated during dynamic loading condition which requires a steady state velocity for compensate the pitching moment due to unsymmetrical pressure development. Figure 6.0 show the statically determinant FBD of the forces acting on the system at any given time frame, which satisfy the needs of

project such that pressure underneath the SKI can be measure by using pressure transducers and co relate with data with velocity profile to validate the theory.

2.2.3 Gantt Chart

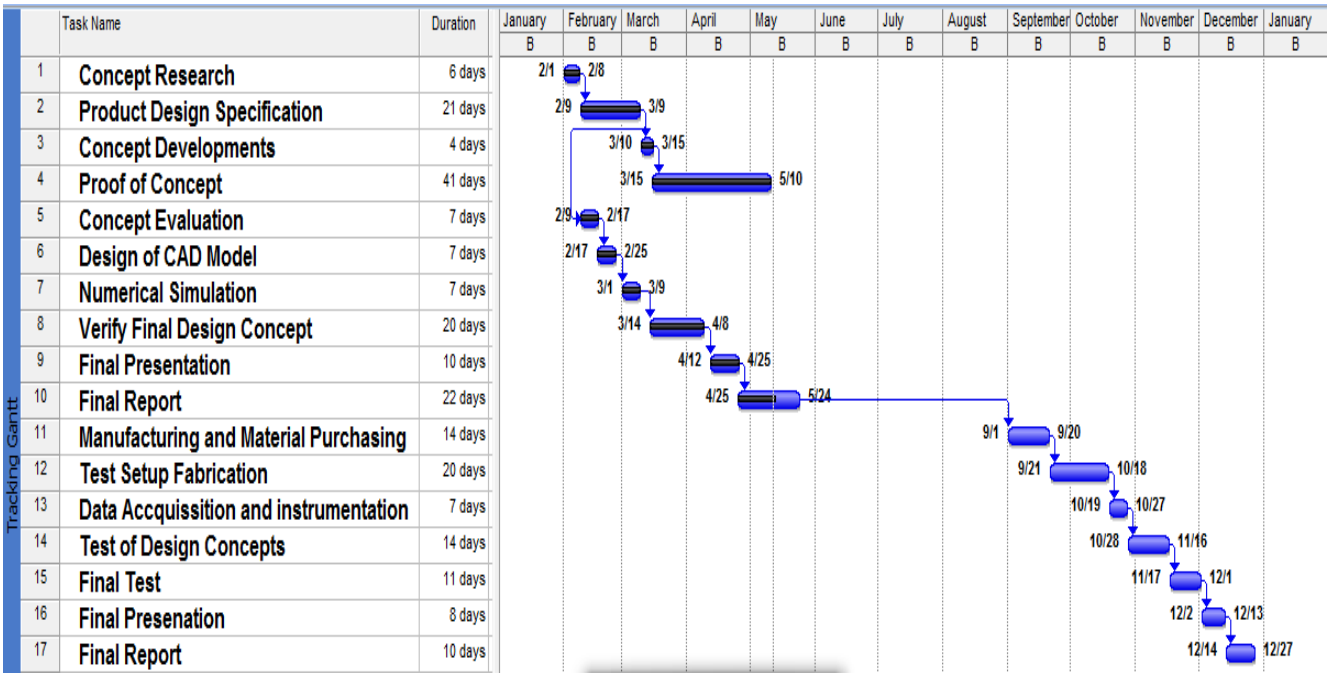

Figure 7.0 Gantt Chart Project work flow diagram

This Gantt chart represents the project management, goals sets and accomplished milestone throughout the time period of the research and experimentation. The project stated with concept research and literature review and followed by the product design specification meeting the customer requirement. The design concepts were developed and evaluated throughout the period of this semester to come up with proof of concepts. For this a CAD model was developed, the mathematically governing equation were numerically solved and the parametric model was reformulated as per the model

For Part II segment of the project, the chart shows the tentative project milestones scheduled for the project. With unexpected financial issues and obligation the most of the phase of experimentation was spend on purchasing and manufacturing the experimental setup. Final testing was done in Early January with proper equipment which yields satisfactory results.

3. Design Concepts

3.1Decomposition into Subsystems

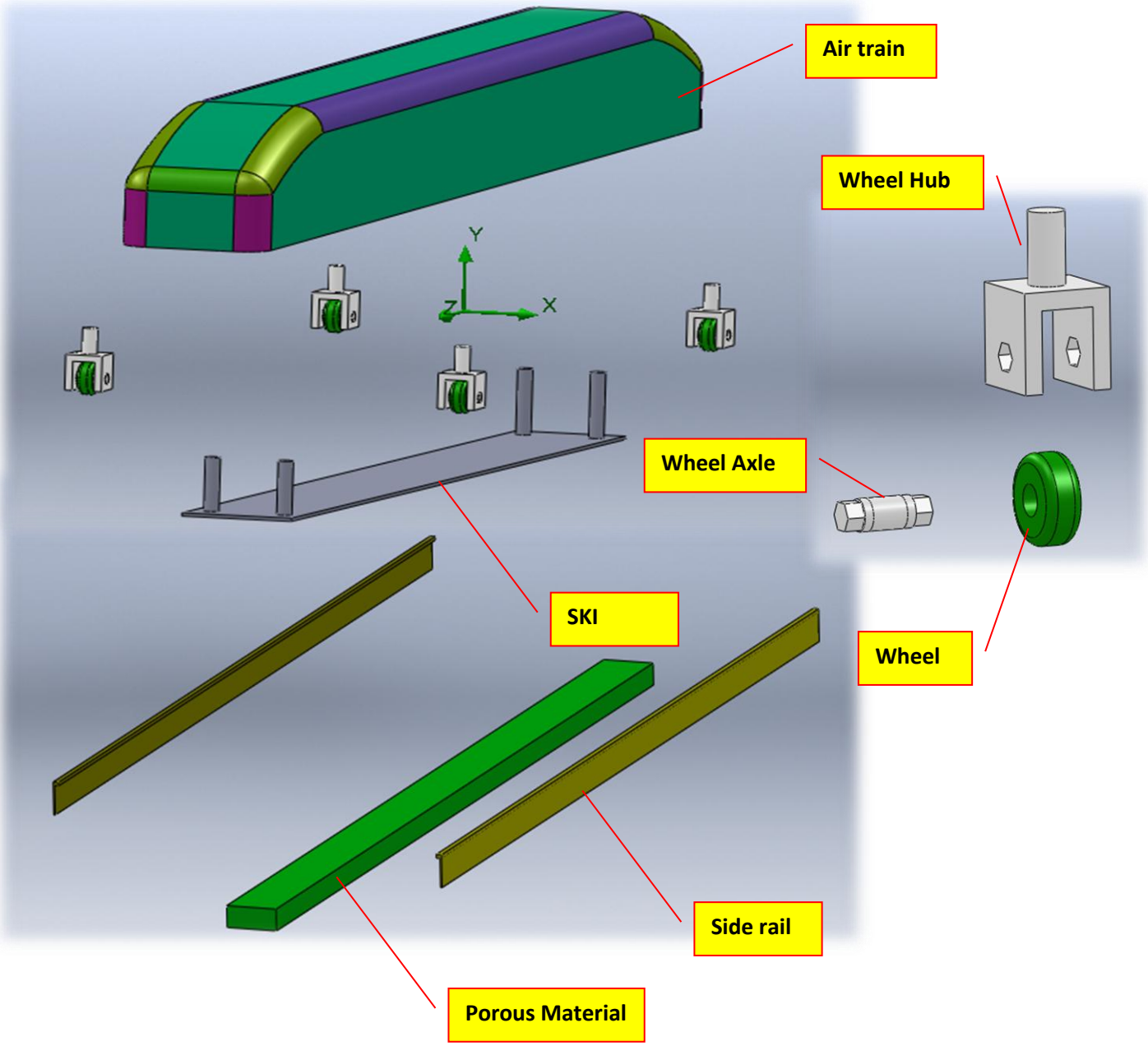

Figure 6.0 Subsystem and Detail Component (data acquisition systems not include)

3.2 Synthesis of subsystems

3.2.1 Mathematical Evaluation

Substituting the equations 1-4 and 6-7 into pressure equation 5,

$$p(x,t) = \frac{\mu U(t) L}{K_p(h_1)} \int_0^{\frac{x}{L}} \frac{-\int_0^1 \frac{1}{\left(\frac{h}{h_1} - \frac{h}{h_1} * \frac{ln\frac{h}{h_1}}{\ln(1-\epsilon)}\right)} \frac{\widetilde{dh}}{\left(1-\frac{h_2}{h_1}\right)}}{-\int_0^1 \frac{1}{\left(\frac{h}{h_1} - \frac{h}{h_1} * \frac{ln\frac{h}{h_1}}{\ln(1-\epsilon)}\right)} \frac{h}{h_1} \frac{\widetilde{dh}}{\left(1-\frac{h_2}{h_1}\right)}} + \frac{h}{h_1}}{\left(\frac{h}{h_1} - \frac{h}{h_1} * \frac{ln\frac{h}{h_1}}{\ln(1-\epsilon)}\right) * \frac{h}{h_1}} \quad (11)$$

$$F_a(x,t) = \frac{1}{A_s} \int_0^L p(x,t) \quad (12)$$

Taking moment about mass center, from equation 10 and 12

$$R_f = \frac{2 * W * L + L * F_a - 6 * F_a * c - L * F_s}{4 * L} \quad (13)$$

$$R_r = W - F_a - R_F - F_S \quad (14)$$

Assumption,

- Negligible change in pressure due to change in height as pressure is function of ratio of differential height over initial thickness.
- Pressure remains constant as soon as the lift occurs, that is air escape at the same rate as the rate of air pushed through the porous materials, and total flux is constant.
- No shear or viscous effect is considered.
- Reynolds number not taken into account for any flow measurement.
- Fibers are aligned perfection in the direction parallel to the flow and hence no accumulation due to viscous effect of flow.

3.2.2 Design Concepts

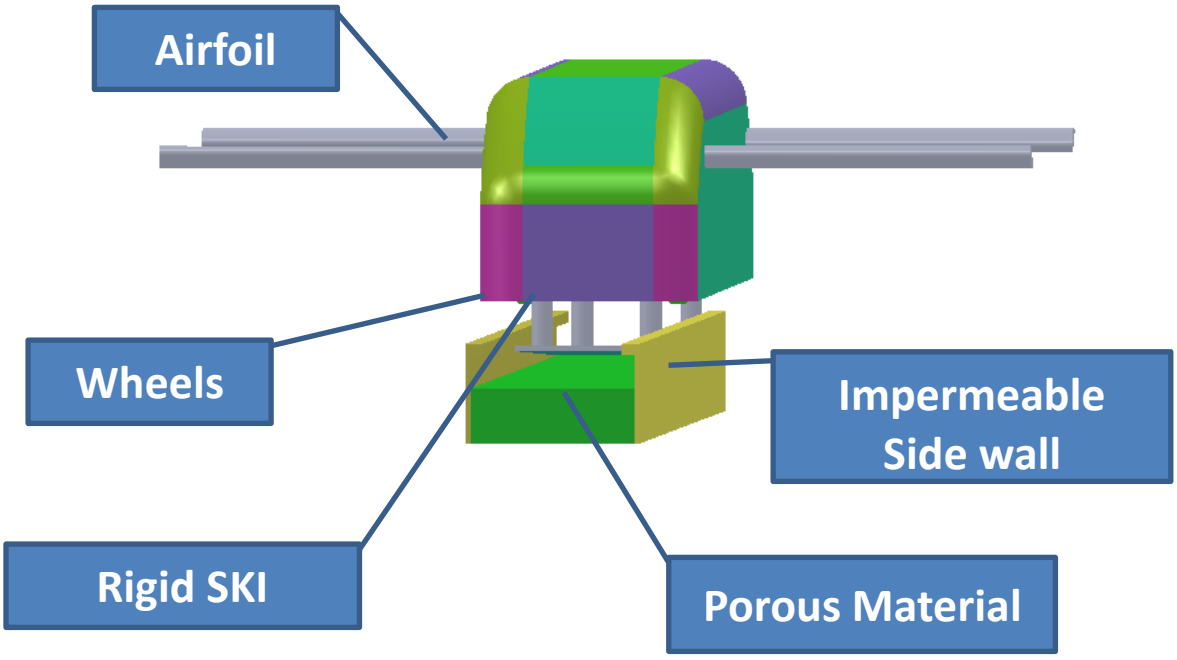

Figure 7.0 Design concepts I (with airfoil)

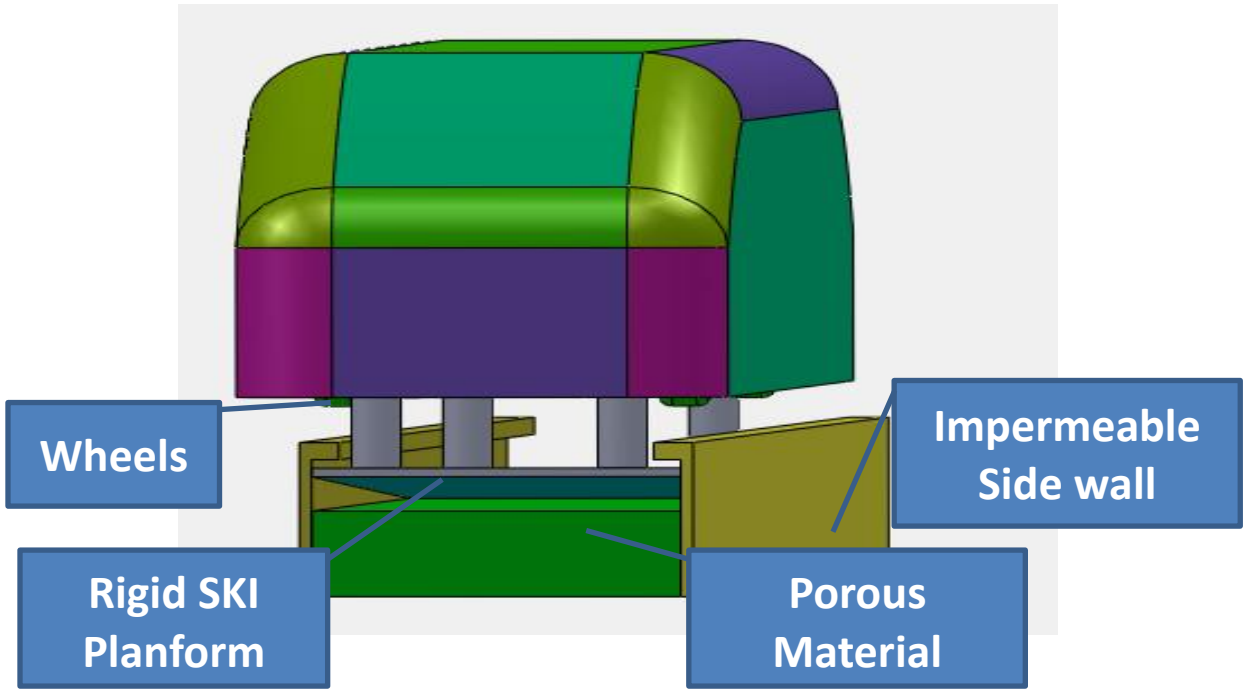

Figure 8.0 Design concepts II (without airfoil)

3.2.3 Decision Matrix

Air Train		
Parameter	Design I	Design II
Manufacturing	+	-
Maintenance	-	+
Cost	-	+
Weight (+)	1	2
Weight (-)	-2	-1
Total Weight	-1	+1

Table 2.0 Decision Matrix

The concept was evaluated in especially three major categories, manufacturing maintenance and cost. For manufacturing the design I was easy as the symmetric body is easy manufacture than design II which need to be model such a way that the mass center is predefine and will be major challenge to be achieve. For maintenance and cost design II is evaluated as easier and better because of the presence of airfoil in design I which yield extra. The total weight was evaluate for both the concept and with close marginal different and space limitation design II was selected as the winner and proposed for the experimentation of the purpose design.

4. Proof of Concepts

4.1CAD Model

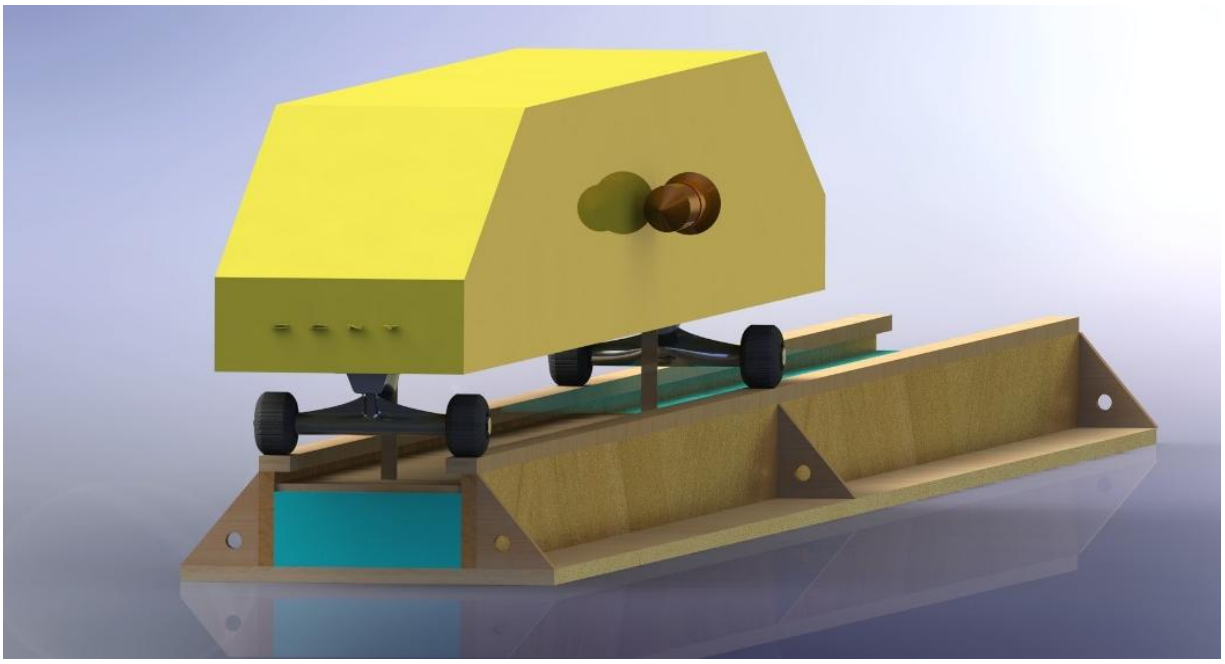

Figure 9.0 3D CAD model of complete Assemble for Design concepts II (without airfoil)

4.2 CAD drawing of subsystems

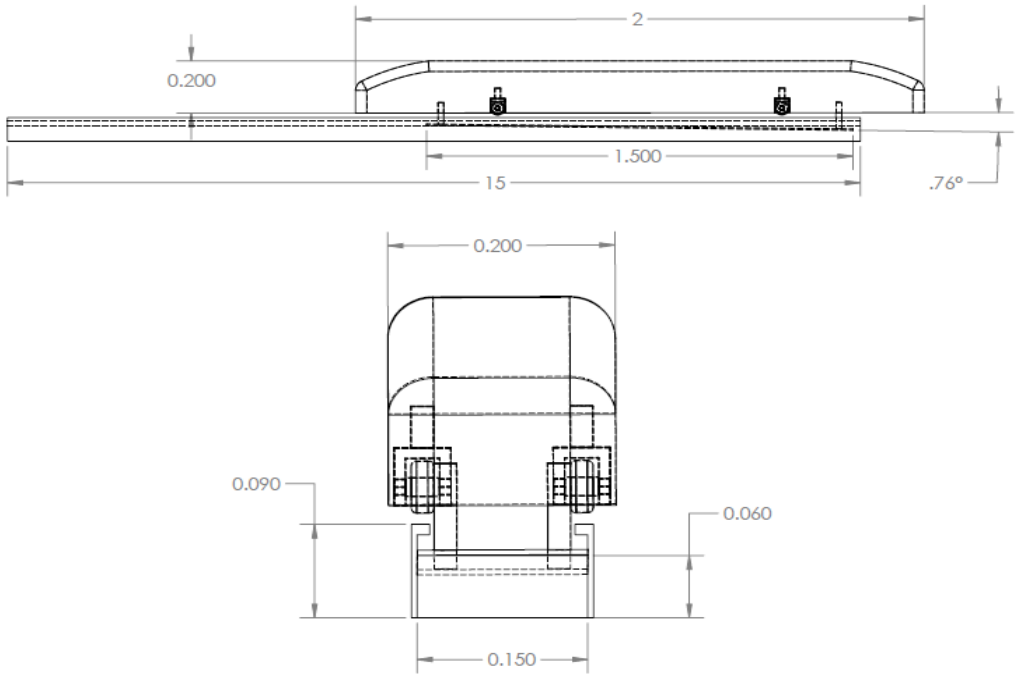

Figure 10.0 2D Sketch of complete Assemble for Design concepts II (without airfoil)

4.3 List of Materials

Train: Plywood
- Easy to workability
- Atheistic finishing surface
- Cheaper

Wheels: Plastics
- Smooth running on the surface
- Cheaper and easily available
- Atheistic finishing surface

Track Side Rail: Plywood
- Low density
- Easy to workability
- Atheistic finishing surface
- Cheaper

Porous Material: Polyester Fibers
- Easily availability
- Cheap
- High permeability
- Fibrous and high void fraction even during compaction
- Small solid compression force

Mesh: Teflon
- Cheap and easily availability
- High porous in respect to mesh surface area
- Low coefficient of friction

Pressure Transducers: Entran Transducers

- High sensitivity
- Dynamic range (0-300 PSI)
- Recycled from previously used experimented at Aero Fluid Lab.

Amplifier: Stanford Research Low Noise Pre Amplifiers SR 560

- Low Noise Fileted
- AC Coupling
- Cut off Frequency (0.03-1 Million)
- Amplification (1-50000)

Data Acquisition: DATAQ DI 710

- 10000 sample/s
- 16 single ended, 8 differential output
- Standalone Recording.
- Memory Card or Computer interface.

5. Results and Discussion

5.1Numerical Results

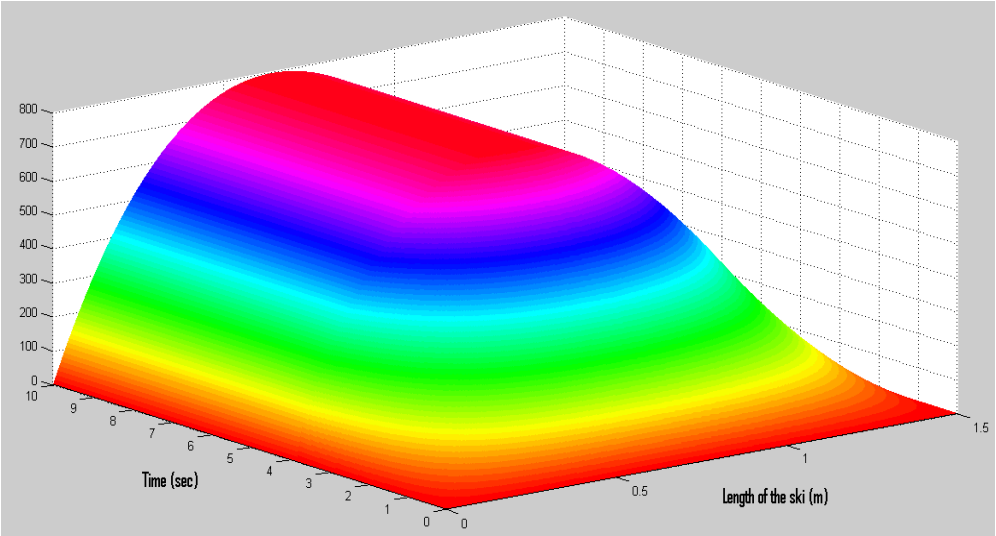

Graph 1.0 Pressure distribution underneath the SKI

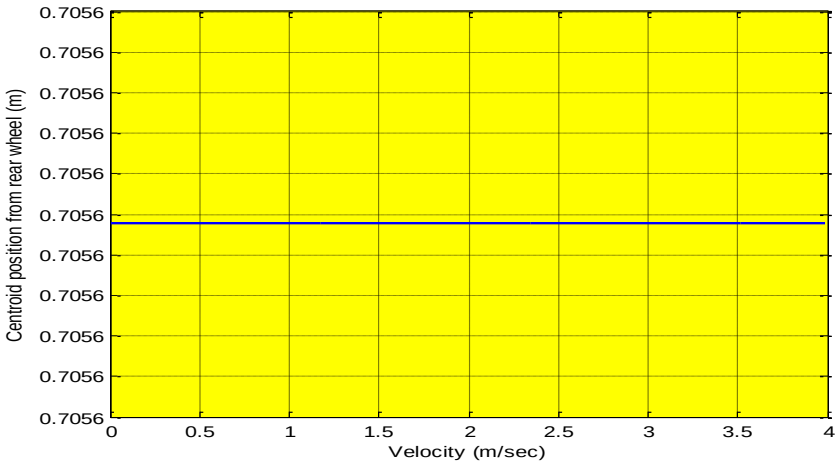

Graph 2.0 Pressure Center plot for pressure curve for different velocity

From the graph 1 above we can see that the pressure distribution curve has a asymptotic solution after time 4 sec which implies that the lift occur for the given design configuration and parameters. The maximum pressure obtain is 800 Pascal with is sufficient enough to lift the train out the track. In graph 2.0 we can see the constant value of the pressure center which depicts that the pressure center in not symmetric but is constant throughout the experimentation period hence the design concept II employed the concept to model the train such that the pressure center and mass center coincidence and eliminate the pitching moment.

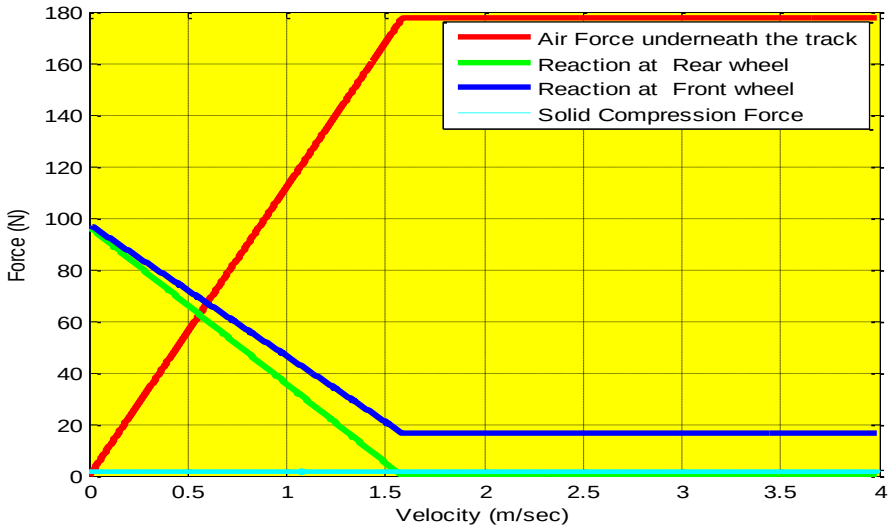

Graph 3.0 Reaction forces plot for different velocity

0 < U < 1.583 m/s

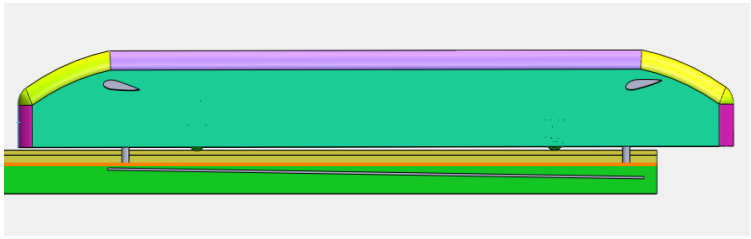

1.58< U < 42.3 m/s

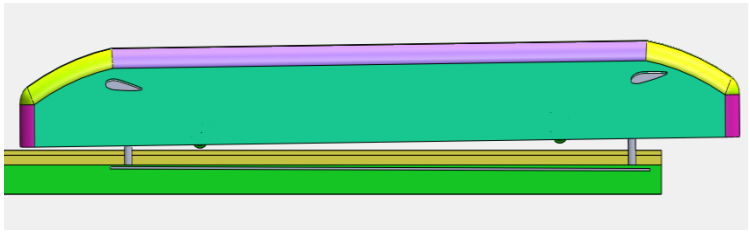

42.31 M/s < U

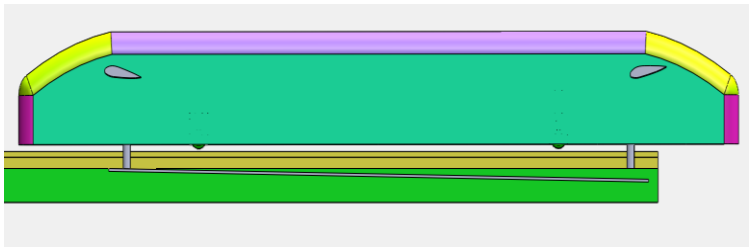

Figure 11.0 State of Operation

From the graph 3, we can see plots of reaction forces and normal forces produce during the dynamic condition. From the graph we can see that the air force is increasing linearly to value close to the weight of the train and as the value get over the weight of the train with move with a constant steady state value. Similarly the reaction forces also

decrease linearly and the air force reach the constant value the reaction force also maintain steady state value. The graph also show that the reaction forces on the front wheel is not zero unlike the rear wheel where the reaction force is zero, which is due to the unsymmetrical pressure distribution curve which produce lift on the rear wheel first. This produces a pitching moment which can be seen on figure 11 where this pitching moment is compensated by the lift produce by the air foil at the front.

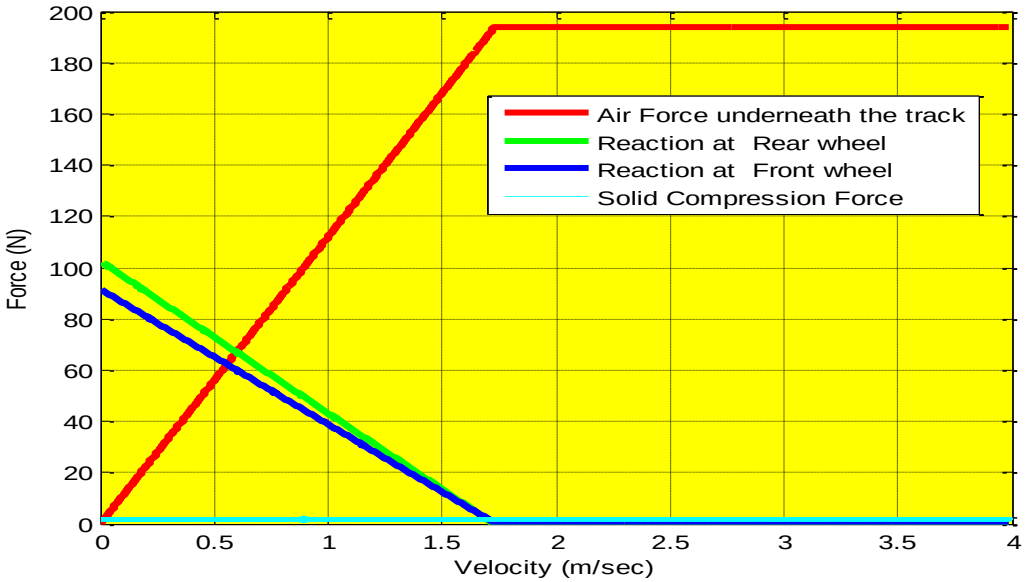

Graph 4.0 Reaction forces plot for different velocity

0 < U < 1.7 m/s

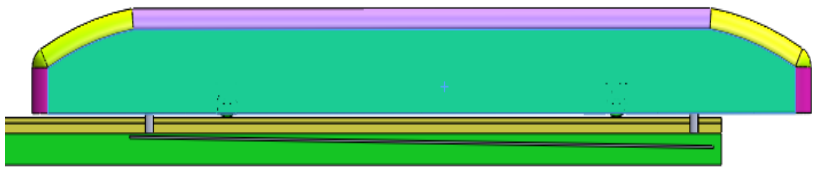

1.7 m/s < U

Figure 12.0 State of Operation

From the graph 3, we can see plots of reaction forces and normal forces produce during the dynamic condition for design concept II which employs the no airfoil concepts however its mass center coincidence with pressure center hence eliminating pitching moment as show in figure 12.0 . From the graph 3 we can see the reaction forces also decrease linearly is zero, and there occur on offset value between two forces.

5.2 FEM analysis

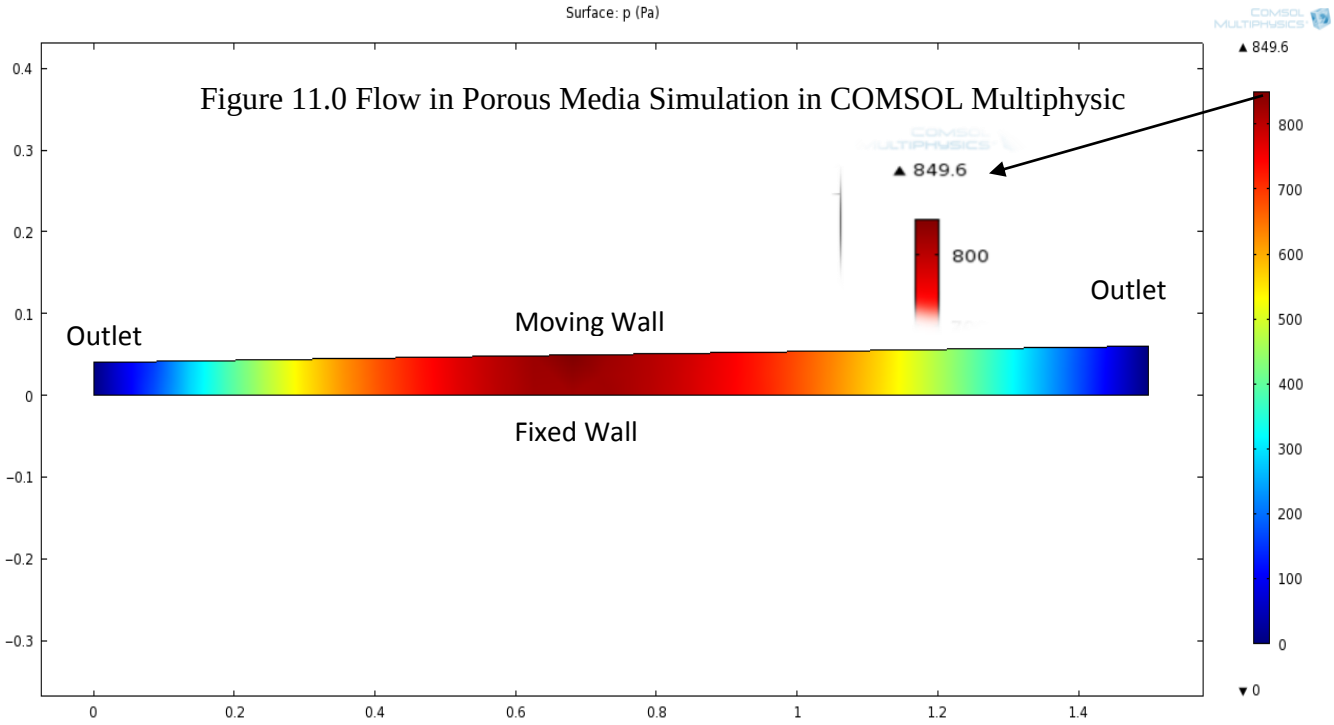

Figure 11.0 Flow in Porous Media Simulation in COMSOL Multiphysic

The numerical result evaluated with numerical solution of equation 10 was crossed checked with computer simulation software COMSOL 3.4, for flow in porous medium package. The geometry of the section of the track covered by the ski at any instance was modeled. The left and right were setup as the outlet boundary as zero gauge pressure. Bottom wall was setup as no slip wall boundary condition and top wall was setup as moving wall at the speed of 1.7 m/s parallel to the ground. This speed was found from the numerical solution as lift speed. A fine triangular mesh size was used to generate mesh. The model took 12 sec to provide the solution, and is as shown in the figure above. The result was off by 50 Pascal as for numerical solution yield 800 Pascal. The software used Brinkman's equation to solve the model and hence uses slightly different approach to the problem; however it is still yet to be verified with experimental result that if the numerical and simulation results make any sense to real world situation.

5.3 Experimental Procedure:

Figure 12.0 System Level Designs

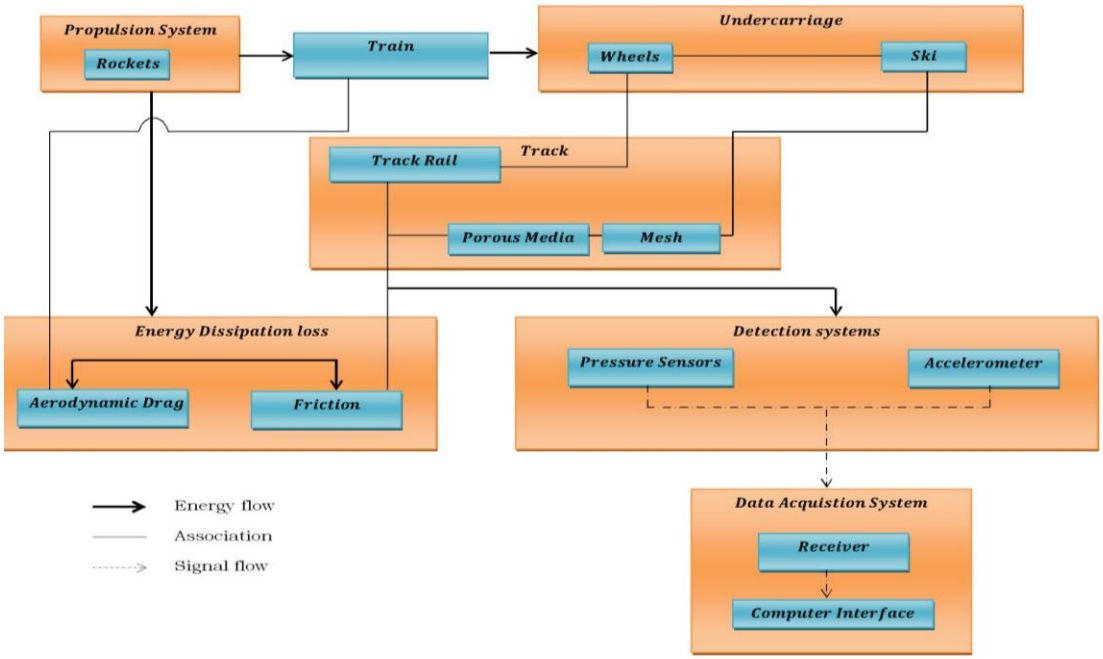

As shown in the above system level diagram gives a detail idea of the system level design of the experimental setup. The Propulsion system powered by rocket to propel the train from one end of the track to other end overcoming friction and drag force along with providing necessary speed to develop the pressure underneath the SKI. The undercarriage of the train is comprised of two component, wheels and SKI. The sensor and detection system was mounted onto the track and electrically wired to the data acquisition system through which data was recorded and analyzed in computer interface.

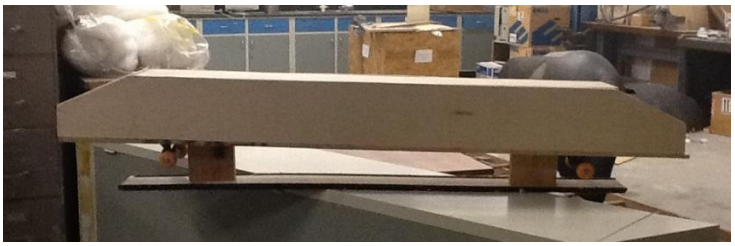

5.4 Stage I Testing and Results:

First stage testing was conduction at chemical engineering lab space at second floor at Steinmann Building. Because of the safety factor the train was pushed manually over the track instead of rocket and signal was acquired through pressure transducer mounted on the base plate of the track. The Pressure Sensor was excited with 5 volts of input current. The signal was then transferred to Amplifier whose filter frequency was setup at 0.03Hz High pass and 100 Hz Low pass and signal was then amplified by factor of 1000. The amplified Signal was then transferred to DATAQ 710 device and to the computer. WQ Real-time Viewer in Oscilloscope mode software was used to view the signal in real time and calibrate the pressure sensor. The software was very handy in recoding and viewing data in real time the data and also had an option to transfer the recorded into .csv format which was converted in .txt in MS Excel and further data analysis was conducted in MatLab using Appendix B.

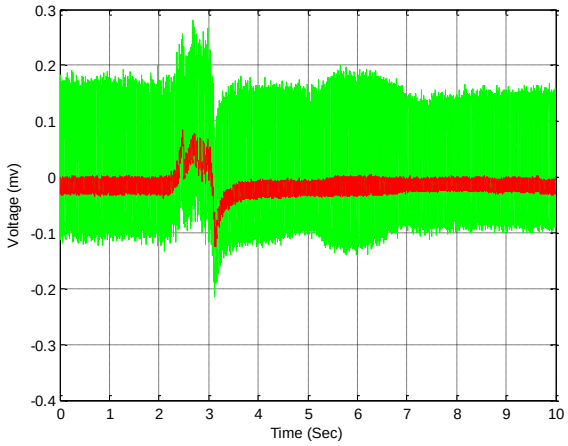

Test 1.0

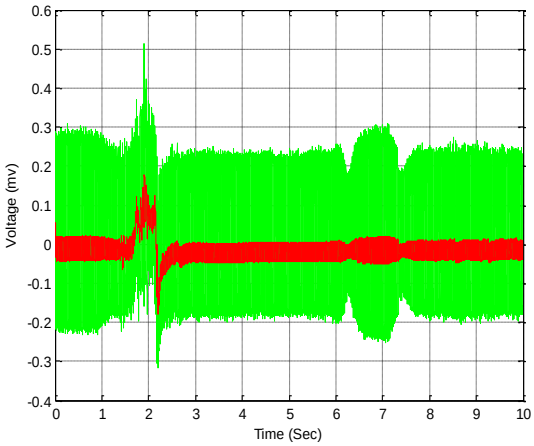

Test 2.0

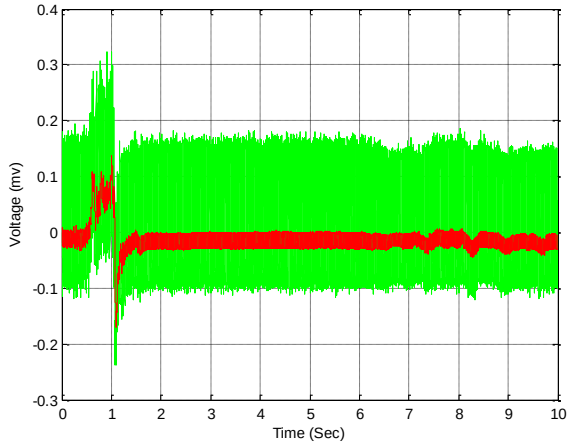

Test 3.0

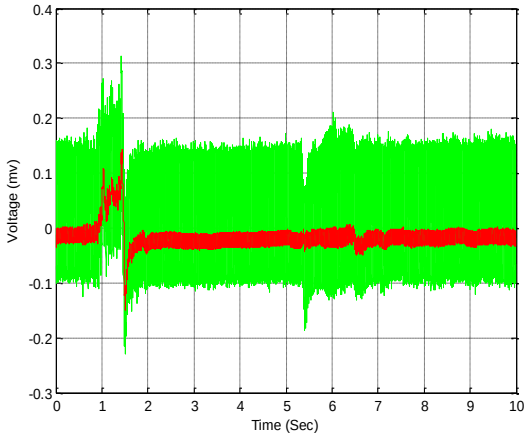

Test 4.0

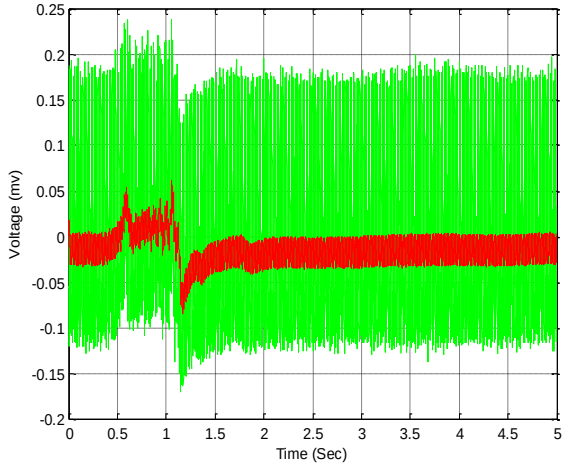

Test 5.0

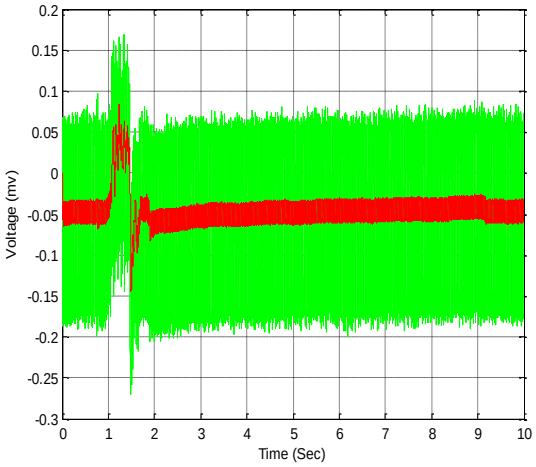

Test 6.0

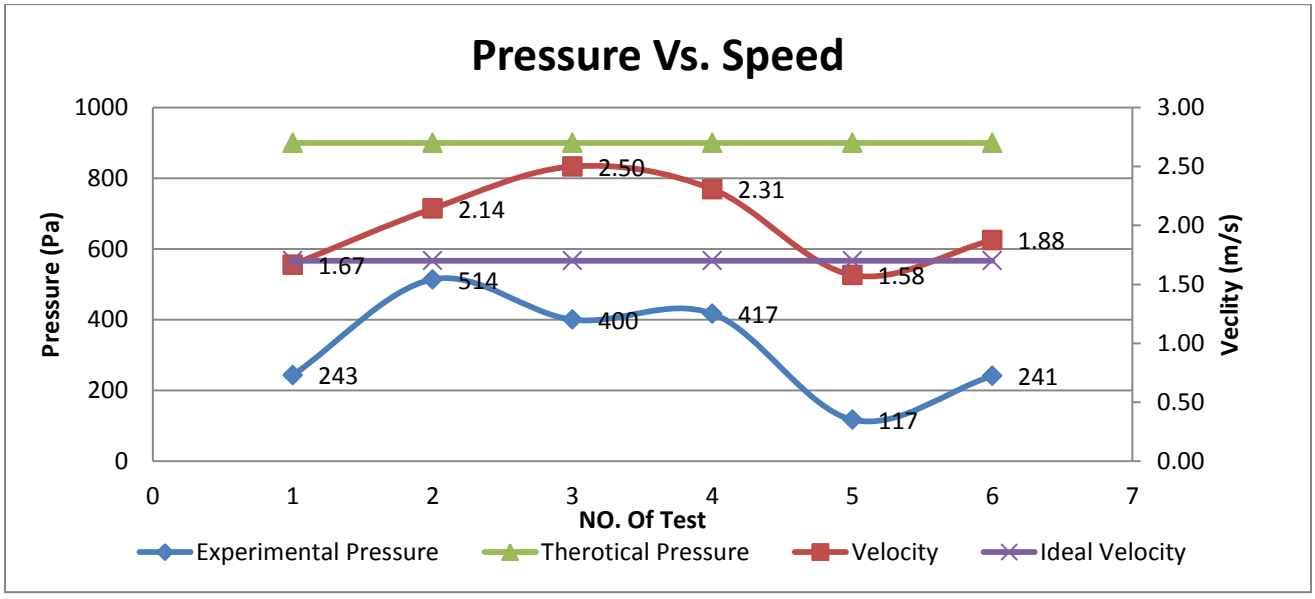

5.5 Problems and Modification:

As from the Test 1-6 we can see the signal has lost of noise compare the actual actuated signal hence it was very difficult to do analysis. Using Butter filter in MatLab the analysis was conducted and the results as shown the graph above show a huge correlation between speed of the train and the pressure. The Green line shows the theoretical pressure develop at speed of 1.7 m/s represented by purple line. However, the blue line which represent experimental pressure and red line represents the corresponding speed. As we can see expect for Experiment no.3 for rest of test run the pressure increases and decreases with respect to the speed of the train and was able to achieve 35 % of the theoretical value. The inefficiency of the experiment could have result from applied filter, excess air leakage and improperly aligned fiber in porous material and also the recovery of porous material. Also it was found that the noise in signal could have come from vibrating floor at 2^{nd} level and also from electrical interference due to presence of huge transformer. Therefore the setup was dismantle and 3/5 length of the track that is 30 feet long track was transfer to cellar level at Air Fluid lab and was assemble again to desired configuration.

5.6 Stage II Testing and Results:

Second stage testing was conduction at Cellar level at Air Fluid lab space in between the wind tunnel and shock tube experimental setup. Because of the safety factor and restriction at lab the train was again pushed manually over the track instead of rocket and signal was acquired through pressure transducer mounted on the base plate of the track. The Pressure Sensor was excited with 5 volts of input current. The signal was then transferred to Amplifier whose filter frequency was setup at 0.03Hz High pass and 100 Hz Low pass and signal was then amplified by factor of 1000. This time to reduce the static noise differential input was setup so the inputs have common ground. The amplified Signal was then transferred to DATAQ 710 device and to the computer. WQ Real-time Viewer in Oscilloscope mode software was used to view the signal in real time and calibrate the pressure sensor. The software was very handy in recoding and viewing data in real time the data and also had an option to transfer the recorded into .csv format

which was converted in .txt in MS Excel and further data analysis was conducted in MatLab using Appendix B.

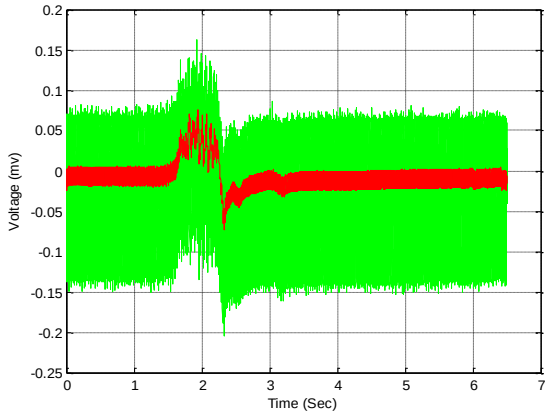

Test 1.0

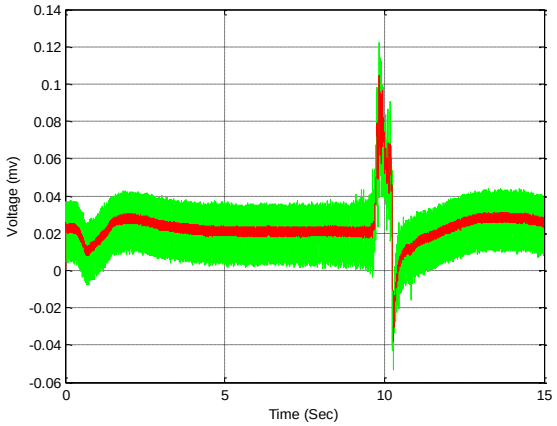

Test 2.0

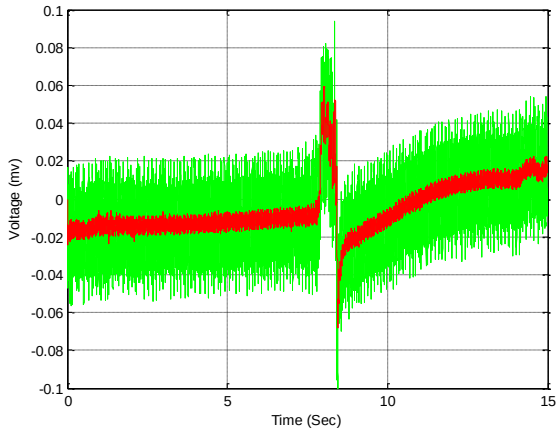

Test 3.0

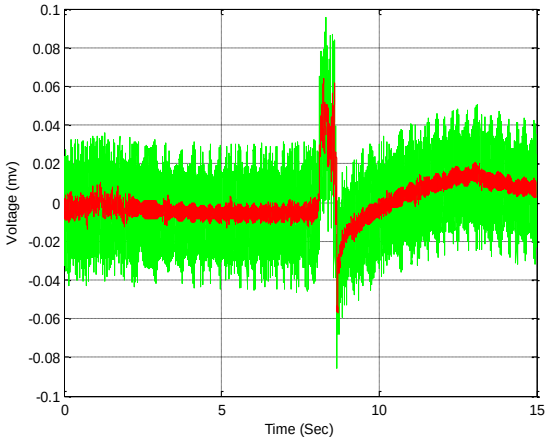

Test 4.0

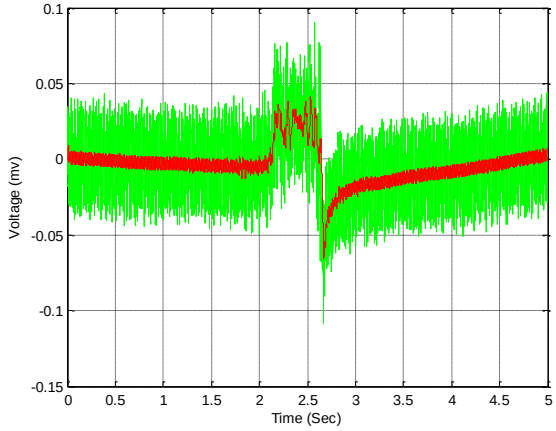

Test 5.0

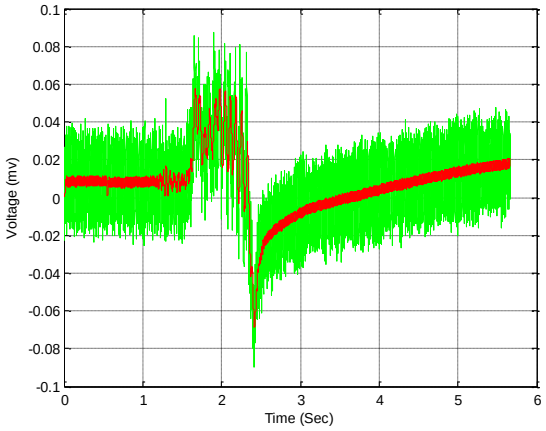

Test 6.0

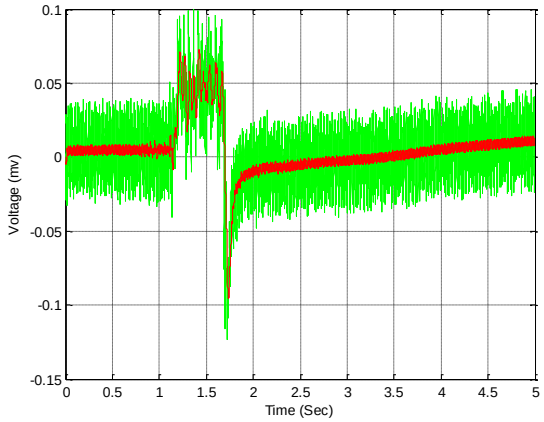

Test 7.0

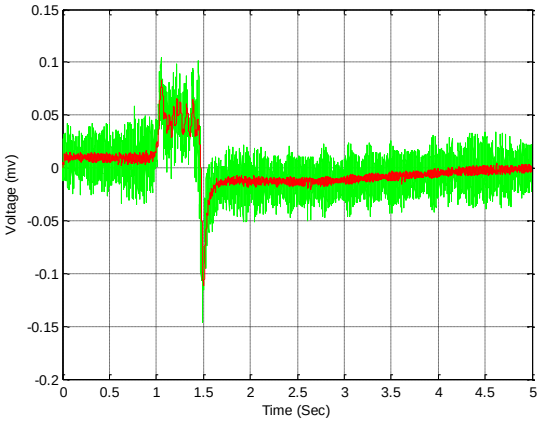

Test 8.0

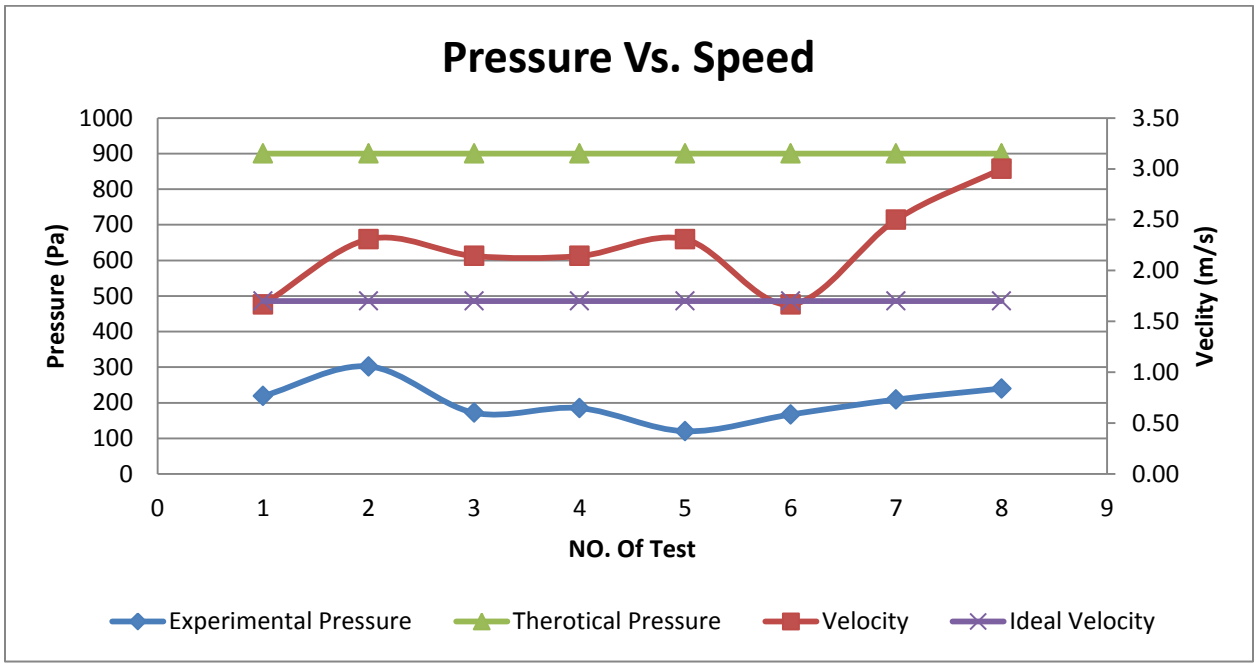

From the test results above we can see the noise is reduce from 1 mv to .05 mv which is exceptionally better quality signal and appropriate in application of filter however the pressure generate at as high as 3 m/s speed was not enough to generate 50 % of theoretical pressure value. Nevertheless the correlation between speed and pressure is validated with fluctuation in the pressure curve with respect to speed of train and are curve are in phase for all case of test runs. Another insight that can be observe from the graph is as the no of experiment increase at higher speed the pressure value is less compare to nearest value of speed at earlier experiment which is because of the material failure to recover 100 percent to its initial phase after each run.

6. Conclusion and Recommendations

Design Concepts:

After careful consideration of the numerical results from data analysis and numerical computation, we can conclude that design 2, the design with no airfoil is better choice when compare not only with stability but also with respect to handle operation, cost of manufacture, and consistence performance. felt that two design concepts best suited the clients' expectations. The first design incorporates airfoils in the front and back of the model. The second alleviates the need for airfoils by shifting the center of gravity over the point of maximum pressure. Figure 11& 12 shows difference between the two designs. Both models, in theory should meet the design requirements so our decisions came down to three parameters; cost, maintenance and manufacturing. Design I, most accurately represents the full scale Jet train concept, and initially was our only consideration. However, when implementing cost and maintenance parameters it was concluded to be disadvantageous when compared to Design II. Cost would be slightly higher when accounting for the extra material and hardware associated adjustable mounts. Maintenance is a concern as well, considering the fragility of the airfoil and the potential for high vibration during acceleration. In addition, the model is expected to endure numerous experiments and any break or shift in the airfoils could give inaccurate results. Design II show greater potential in cost and maintenance due to less material and no upkeep associated with the airfoils. Manufacturing could be a concern due to the effort involve with shifting the center of gravity, but overall seemed less significant.

Material Selection:

The material selected for our design is based on the design specification and numerical calculations. We chose plywood for construction of train and track which was explicitly demanded by the sponsor. However working with plywood was initially ease however as the construction of track came in front, the twist and deformed wood plank was much harder to handle in alignment of track than expected. Hence, is not recommended for any future work. SKI which has to be precisely at desired angle of attack and nearly frictionless, the plywood SKI performance was not efficient as desired. ½ inch thick Plywood was used which increased the contact area between the side rails hence create more vibration friction and caused air leakage. Porous material, was tested in prod experiment hence performed very well as expected, which was considered from previous studies, is a polyester fiber. However, any future work should take considered regarding the recovery property of fiber material as it was observed that after 3-4 run the recovery of porous material reduce largely. Lastly, meshing that allows air to move freely is needed to cover the porous material. Based on the results, Teflon was that material of choice because of its low friction coefficient and breathability.

Thrust and Pressure:

Proper acceleration and velocity is required to generate the desired 800 Pascal of air pressure underneath the SKI Planform. Given the space stated in the design specification, thrust was major concern with our design. Initially a small jet engine was considered for acceleration and velocity requires but cost, safety and complexity of such a component didn't seem feasible. Solid state disposable rockets generating around 8 N forces was a better option, however still debatable. In any case, we expect lift to occur at 1.7 [m/s] after 3.7 [m] displacement and need to base the propulsion system on these results. However due to safety and restriction in lab consideration manual push was used to propel the train which is less precise with respect to the creation of secondary force to improper push which creates initial pitching moment of vibration as well.

Future Recommendation:

The design should take consideration mass is uniformly position such that CG coincidence with pressure center. Longer test tracks with train designs that explore real world conditions can be expected and ultimately leading up to a full scale Jet train prototype. Longer tracks so the train reaches some stability rather than taking data immediately after the initial impulse. The porous material should be change after 3-4 runs so the recovery is consistence in multiple test run. The experiment should be conducted in open space outdoor for the use of rockets for safety concerns. New Pressure sensors are required as the recycle sensors are inconsistence in performance and most of them are not in working condition. And sensor should be bought that satisfy our need of range that is 0-5 psi miniature sensor. It is recommended to use steel or aluminum for construction of train and track as they have less issue with alignment and twist unlike wood. SKI should be made of thin rigid aluminum sheet. The wire should be connected via soldering rather just connecting and taping. Soldering reduce resistance and chance of short circuiting. Exposed wire should be cover with aluminum foil to reduce antennae effect as the exposing sire taken interfere signal as well. The area of data should be electrical noise free and all power devices should have common ground. The location of Pressure sensor on the track should be vibration free to avoid any initial noise.

7. Acknowledgement

Though a great effort individually and firm group works efforts invested in this project it would not have been possible without the kind support and help of many individuals. Therefore we would like to extend our sincere thanks to all of them.

We are highly indebted to Prof. Charles B. Watkins and Prof. Yiannis Andreopoulos for his guidance and constant supervision as well as for providing necessary information regarding the project & also support in completing the project. We would also like to express our special gratitude towards Mr. Akaydin Dogus Ms. Parisa Mirbod for their kind co-operation and insights which help us in completion of this project.

I would like to express my special gratitude and thanks to Mr. Chen for giving us attention and time for technical help.

Our thanks and appreciations also go to our colleague in developing the project and people who have willingly helped me us with their abilities.

8. Reference

[1] Wu, Qianhong, Andreopoulos Yiannis, and Weinbaum Sheldon. "From red Cells to snowboarding: A New Concept for a Train Track" *Physical review Letters.* 93.19 (2004): 194501.Print.

[2] Mirbod, Parisa, Andreopoulos Yiannis, and Weinbaum Sheldon. "Application of Soft Porous Materials to a High-Speed train track." *Journal of Porous Material*. 12.11 (2009): 1037-52. Print.

[3] Mirbod, Parisa, Andreopoulos Yiannis, and Weinbaum Sheldon. "On the Generation of Lift Forces in Random Soft Porous Media." *Journal of Fluid Mechanics*. 619 (2008): 147-66. Print.

[4] Crawford, Robert, Gerard F . Jones, Lidan You, Qianhong Wu. "Compression-Dependent Permeability Measurement for Random Soft Porous Media and its Implication of Lift Generation" *Chemical Engineering Science.* 66 (2011): 294-02.Print.

[5] Popescu, Cristian S. "Dynamic Permeability of Highly Compressible Porous Layers under squeeze at Constant Velocity and under Impact " *Tribology International.* 44 (2011): 272-83.Print.

9. Appendix A

```
% High Speed AJT
% Group Name: Transrapid Racer

clear all
close all
clc

prototype_length_train = 40;      % meters
prototype_width_train = 4;        % meters
prototype_height_train = 4;       % meters
prototype_length_ski = 30;        % meters
prototype_width_ski = 3;          % meters

% Model Specification
scale_factor =1/20;                                                 % Geometric
dimensional scale factor
model_length_train = scale_factor*prototype_length_train;      % m
model_width_train = scale_factor*prototype_width_train;        % m
model_height_train = scale_factor*prototype_height_train;      % m
model_length_ski = scale_factor*prototype_length_ski;          % m
model_width_ski = scale_factor*prototype_width_ski;            % m
coff_drag=0.2;                                                      % sphere
model_cross_sec_area=model_width_train^2;                           % assuming
spherical cross section

% Environment
temp=20;                                                            % Celcius
density_air=1.117;                                                  % kg/m^3
viscosity=1.78*10^-5;

% Material
mass_train=20;                                                      % kg
weight_train=mass_train*9.81;                                       % N

% Propulsion System
No_iteration=1000;
final_time=10;
step_size_time=(final_time-0)/No_iteration;
t=0:step_size_time:final_time;

% Propulsion System
thrust=8;
velocity=sqrt(thrust/(0.5*coff_drag*density_air*model_cross_sec_area))*tanh(s
qrt(0.5*coff_drag*density_air*model_cross_sec_area*thrust)*t/mass_train);
velocity_final=velocity(1,No_iteration+1);

% SPT Model
permeability_poly=3.4*10^-9;
% material used as porous media polyester k_p (m^2)
SPT_thickness_leadingedge_ski=.06;
% height of uncompressesd track (m)
```

```
SPT_thickness_trailingedge_ski=.04;
% height of uncompressesd track (m)
% width of uncompressesd track (m)
angle_attack=atan((SPT_thickness_leadingedge_ski-
SPT_thickness_trailingedge_ski)/model_length_ski);              % slope of
ski
angle_attack_degree=angle_attack*180/pi;
compression_ratio
=SPT_thickness_leadingedge_ski/SPT_thickness_trailingedge_ski;
% compression ratio

% Dimensionless parameter
% Length of SKI
step_size_ski=(model_length_ski-0)/No_iteration;
Length_step_size=0:step_size_ski:model_length_ski;
dimless_length=Length_step_size./model_length_ski;

% Thickness of SPT
compressed_thickness=(SPT_thickness_leadingedge_ski-
SPT_thickness_trailingedge_ski).*dimless_length+SPT_thickness_trailingedge_sk
i;
dimless_thickness=compressed_thickness./SPT_thickness_leadingedge_ski;

% Permiability of Material
permiability_material_uncompressed=3.4*10^-9;
void_fraction=0.995;
dimless_permiability=dimless_thickness-
(dimless_thickness.*log(dimless_thickness))/(log(1-void_fraction));

% Pressure
a_int=SPT_thickness_trailingedge_ski/SPT_thickness_leadingedge_ski;
a_fin=SPT_thickness_leadingedge_ski/SPT_thickness_leadingedge_ski;
step_size_coff=(a_fin-a_int)/No_iteration;
coff_step_size=a_int:step_size_coff:a_fin;
Coff_1=trapz(coff_step_size,-
1./dimless_permiability)./trapz(coff_step_size,1./(dimless_permiability.*diml
ess_thickness));

% Pressure Distribution
Pressure_1=(viscosity*model_length_ski.*velocity)./(permiability_material_unc
ompressed);
Pressure_2=(-
(Coff_1+dimless_thickness)./(dimless_permiability.*dimless_thickness)).*SPT_t
hickness_leadingedge_ski/(SPT_thickness_leadingedge_ski-
SPT_thickness_trailingedge_ski);
pre_1(1,1)=0;
for a=1:1:No_iteration

pre_1(1,a+1)=pre_1(1,a)+step_size_coff*(Pressure_2(1,a)+Pressure_2(1,a+1))/2;
end
pre_1(1,No_iteration+1)=0;

Pressure_3=Pressure_1'*pre_1;

for b=1:1:No_iteration+1
```

```
    test_pressure=Pressure_3(b,1:No_iteration+1);

centroid(1,b)=trapz(Length_step_size,test_pressure.*Length_step_size)/trapz(L
ength_step_size,test_pressure);
    Pressure_int(1,b)= trapz(Length_step_size,test_pressure);
end

delta_height=(SPT_thickness_leadingedge_ski-
compressed_thickness)./SPT_thickness_leadingedge_ski;

Solid_pressure=142.5*(model_length_ski*model_width_ski).*delta_height;

Solid_force=trapz(Length_step_size,Solid_pressure.*(model_length_ski*model_wi
dth_ski));

Air_force=Pressure_int.*(model_length_ski*model_width_ski);

% Moments About the Centroid

Reaction_front=(2*weight_train*model_length_ski+model_length_ski.*Air_force-
6.*Air_force.*centroid-model_length_ski.*Solid_force)/(4*model_length_ski);
Reaction_rear=weight_train-Air_force-Reaction_front-Solid_force;

for c=1:1:No_iteration+1
    if Reaction_rear(1,c)>=0
        Reaction_rear(1,c)=Reaction_rear(1,c);
        p=c;
    elseif Reaction_rear(1,c)<0
        Reaction_rear(1,c)=0;
        Reaction_front(1,c)=Reaction_front(1,p);
        Air_force(1,c)=Air_force(1,p);
        Pressure_3(c,:)=Pressure_3(p,:);
    end
end

lift_speed=velocity(1,p);
lift_time=t(1,p);
velocity_max=velocity(1,No_iteration);
distance_lift=0.5*lift_speed*lift_time;
distance_final=0.5*velocity_final*final_time;


disp('************* AIR TRAIN *******************************')
disp('The  scale factor of the model is'),disp(scale_factor)
disp('The Length of the 1/20 scale model of train is:(meters)
'),disp(model_length_train)
disp('The width of the 1/20 scale model of train is:
(meters)'),disp(model_width_train)
disp('The height of the 1/20 scale model of train
is:(meters)'),disp(model_height_train)
disp('The Length of the 1/20 scale model of ski is:(meters)
'),disp(model_length_ski)
disp('The width of the 1/20 scale model of ski is:
(meters)'),disp(model_width_ski)
disp('The mass of the 1/20 scale model of train is:(kg)'),disp(mass_train)
```

```
disp('The lift speed of the air train is: (m/s)'),disp(lift_speed)
disp('The time to reach lift speed'),disp(lift_time)
disp('The distance cover by the model at lift'),disp(distance_lift)
disp('The distance cover by the model'),disp(distance_final)
disp('The maximum velcoity reached'),disp(velocity_max)


disp('************Soft Porous Track Model************************')
disp('The permeability of the material: (m^2) '),disp(permeability_poly)
disp('The width of the 1/20 scale model of train width is:
(meters)'),disp(model_width_ski)
disp('The height of the SPT at front end of ski
(meters)'),disp(SPT_thickness_leadingedge_ski)
disp('The height of the SPT at rear end of ski (meters)
'),disp(SPT_thickness_trailingedge_ski)
disp('The angle of attack for ski is: (degrees)'),disp(angle_attack_degree)
disp('The compression ratio of the train: '),disp(compression_ratio)

figure(1)
plot(t,velocity,'r-')
grid on
xlabel('Time(sec)')
ylabel('Velocity (m/s)')
title('Velocity of 1/20 scale model of AJT')

figure(2)
% Length of SKI
surf(Length_step_size,t,Pressure_3,'EdgeColor','none')
title('Pressure Distribution')
xlabel('Length of the ski (m)')
ylabel('Time (sec)')

figure(3)
% Force Balance
plot(velocity,Air_force,'r-',velocity,Reaction_rear,'g-
',velocity,Reaction_front,'b-',velocity,Solid_force,'c-')
grid on
xlabel('Velocity (m/sec)')
ylabel('Force (N)')
legend('Air Force underneath the track','Reaction at  Rear wheel','Reaction
at  Front wheel','Solid Compression Force')
```

Appendix B

```
clear all
close all
clc

const_pa_psi=0.000145;
required_Pa=900;

b=load('Final test 19 move.txt');

Run1=b(:,1:2);
exp1=Run1;
exp1(:,2)=-1.*exp1(:,2);


order=2;
sampling_frequency=4800;
cut_off_frequency=24;
[B1 A1]= butter(order,0.02);%cut_off_frequency/(sampling_frequency/2));
y1=filter(B1,A1,exp1(:,2));


figure(1)
plot(exp1(:,1),exp1(:,2),'g-')
hold on
plot(Run1(:,1),y1,'r-')
xlabel('Time (Sec)')
ylabel('Voltage (mv)')
grid on
hold off

% Calibration Eequation y = 2.4*x + 1.3e-014;
exp1x= max(y1);
exp1y=(0.42*exp1x + 4.7e-15)/const_pa_psi;

disp('The Peak Pressure Experiemntal Test 1 is (Pa): ')
fprintf( ' %10.3f \n ', exp1y)
disp('The Peak Pressure Theoritical is (Pa): ')
fprintf( ' %10.3f \n ', required_Pa)
```

Appendix C

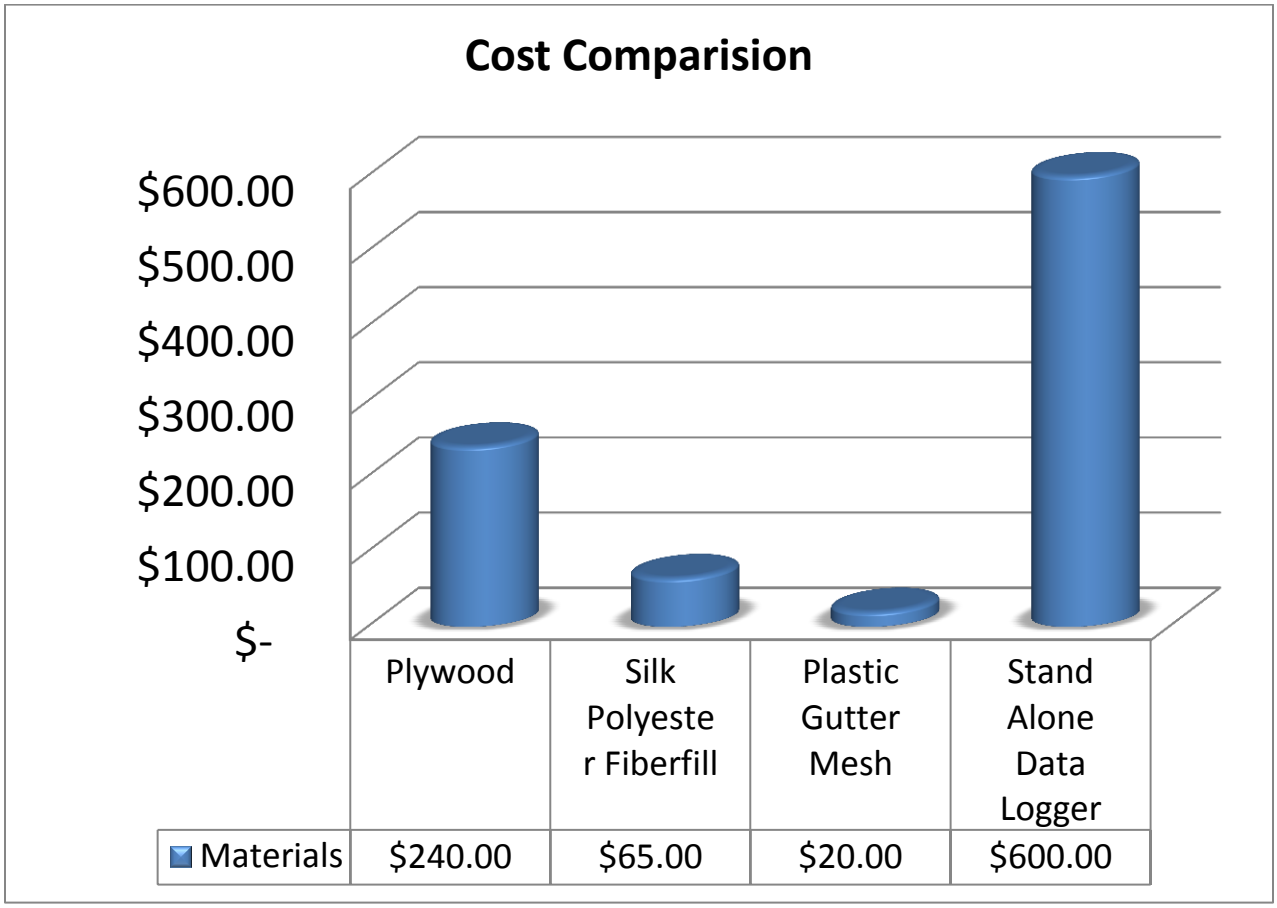
Cost Comparision
$600.00
$500.00
$400.00
$300.00
$200.00
$100.00
$-
Plywood
Silk Polyester Fiberfill
Plastic Gutter Mesh
Stand Alone Data Logger
Materials
$240.00
$65.00
$20.00
$600.00

Appendix D

Data Acquisition

Stand-Alone Data Logger	
	
Vendor	Cost
Dataq Instruments	$607

Mesh

PVC 20 Gauge 1 inch Mesh	
	
Vendor	Cost
Amazon.com	$20.00

Porous Material

A Touch of Silk Fiberfill	
	
Vendor	Cost
Mountain- Mist	$64.48

Track and Train Body

Maple Ply-Wood	
	
Vendor	Cost
Tulnoy Lumber	$231.80